Preliminary Study on the Candidate Fuel Salt of Molten Chloride Salt Fast Reactor

Sungtaek Hong[ab], Seongdong Jang[b], Taesuk Oh[b] and Yonghee Kim[b*]
[a]*Korea Atomic Energy Research Institute, 111, Daedeok-daero 989beon-gil, Yuseong-gu, Daejeon, Republic of Korea*
[b]*Korea Advanced Institute of Science and Technology, 291 Daehak-ro, Yuseong-gu, Daejeon, Republic of Korea*
[*]*Corresponding author: yongheekim@kaist.ac.kr*

1. Introduction

The Molten Salt Reactor (MSR) is one of the Generation IV International Forum (GIF) nuclear reactor systems [1], and it provides unique unparalleled advantages such as low pressure operation, liquid fuel and very high fuel utilization, etc. However, the conventional thermal spectrum-based MSRs require moderator, which is often the graphite that results in the periodic production of radioactive waste due to short lifetime (4~5 years), and the compulsory on-line removal of fission-products incurs proliferation issues. In addition, an ultra-high enrichment of Li-7 in the old F-based molten salts is also a hurdle for development. To overcome the aforementioned drawbacks, an interest toward the fast spectrum based MSRs is being recognized [2].

In this paper, a conceptual study of chloride-based long-life fast-spectrum MSR utilizing low-enriched U-235 is presented. It is worthwhile to highlight that fluoride-based salts are not preferable for fast spectrum due to their limited solubility for TRUs. The characteristics of KCl-UCl_3 salts and $NaCl$-UCl_3, two possible salt candidates, are investigated along with the general property of the proposed reactor design.

2. Reactor model and fuel salts

2.1 Reactor model

Table 1 shows major design parameters of a simplified integral MSR and Figure 1 shows its conceptual configuration. An integral reactor module is submerged in a containment non-fuel molten salt pool, as shown in Figure 1. Fuel salt is only loaded in the Hastelloy-N reactor vessel. It should be noted that Figure 1 is not to scale and compact heat exchangers are supposed to be placed above the active core region. The active core height is 5 m in the current work.

Table 1. Reactor description (D=diameter, H=height)

Power	400 MWth
Candidate Fuel salt	KCl-UCl_3 / $NaCl$-UCl_3
Reactor vessel (RV) dimension	D=2.5m, H=11.6m
RV structural material	Hastelloy N
Shield material	B_4C
Containment dimension	D=4.7m, H=14.4m
Containment material	SS 304

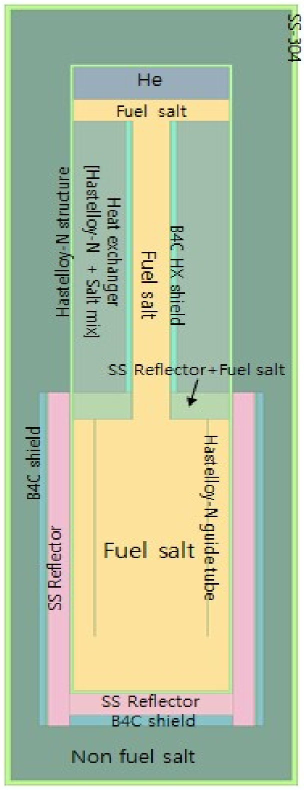

Figure 1. Reactor model (X-Z plane)

2.2 Characteristics of the candidate fuel salts

The first candidate for fuel salt is a KCl–UCl_3 system, which exhibits two eutectic temperature as shown in Fig. 2 [3]. For procurement of high enough fuel inventory, the eutectic temperature at 54 mol% UCl_3 was selected in the presented study. At such solubility, KCl–UCl_3 system has a eutectic temperature with T = 831K (558°C).

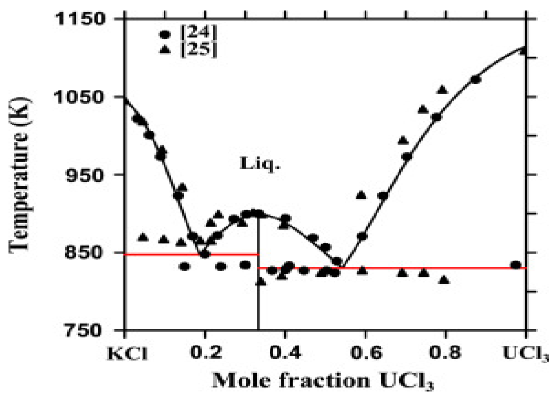

Figure 2. Phase diagram of a KCl-UCl3 system

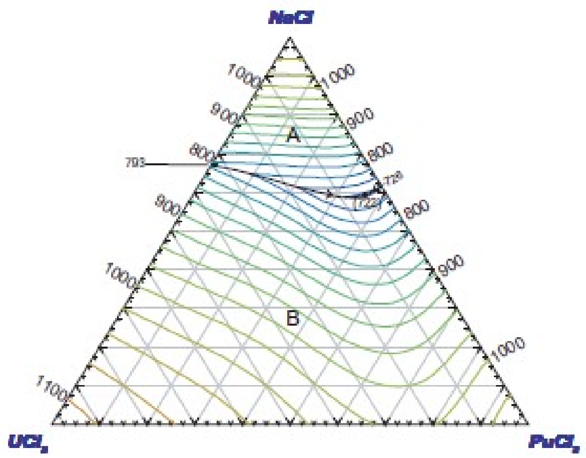

Figure 3. Phase diagram of a NaCl-UCl3 system

The second candidate fuel salt is a NaCl–UCl_3 system. Figure 3 illustrates a eutectic temperature of the NaCl-UCl_3 system, where a eutectic temperature of T = 793K (520°C) occurs at X_{UCl3} = 0.33 [4]. The NaCl–UCl_3 system has a lower eutectic temperature compared to the KCl–UCl_3 system, but exhibits a lower solubility of UCl_3 than the KCl–UCl_3 system.

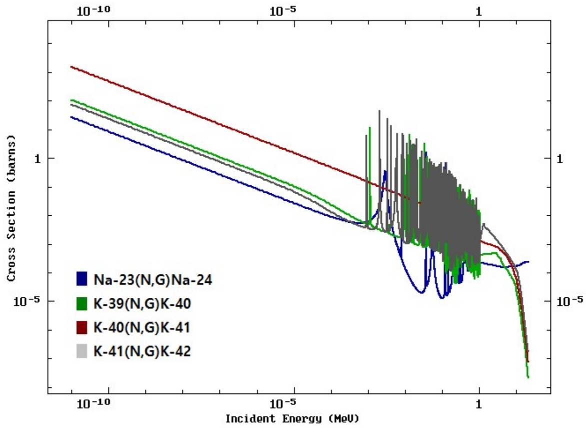

Figure 4. Capture cross section of Na, K

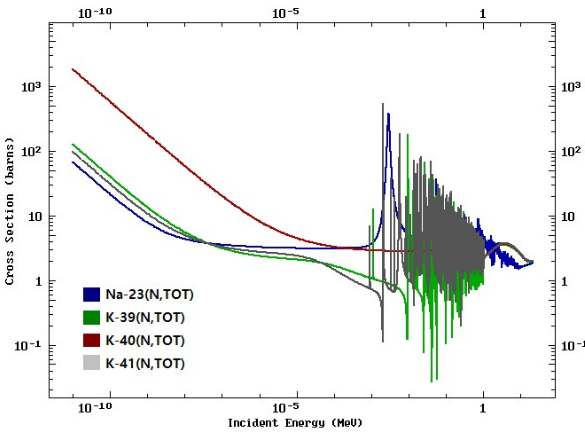

Figure 5. Total cross section of Na, K

Figures 4 and 5 depict the cross sections of Na-23, K-39, K-40, K-41 [5]. The Na-23 has relatively smaller capture cross section in the high energy region, but exhibits a relatively high resonance region at the 1~10 keV neutron energy.

2.3 Criticality calculation

For reactor analysis, both SERPENT Monte Carlo code and ENDF/B-VII.1 cross section library were exploited [6]. The initial U-235 concentrations to achieve criticality were estimated for the aforementioned fuel salts at their eutectic solubility, and the conversion ratio during the operation was also calculated.

Figure 6 shows the neutron spectrum of each fuel salts, where two fuel salt candidates have similar neutron spectrum behavior. Table 2 demonstrates the comparison results between the two fuel salts. The NaCl-UCl_3 system has a lower melting point than the KCl-UCl_3 system, however, the KCl-UCl_3 system has higher solubility of UCl_3 than the NaCl-UCl_3 system at the eutectic temperature. Due to the high solubility of UCl_3 in the KCl-UCl_3 system, initial criticality can be met with a lower U-235 concentration compared to the NaCl-UCl_3 system. In addition, the KCl-UCl_3 system shows a higher conversion ratio than the NaCl-UCl_3 system.

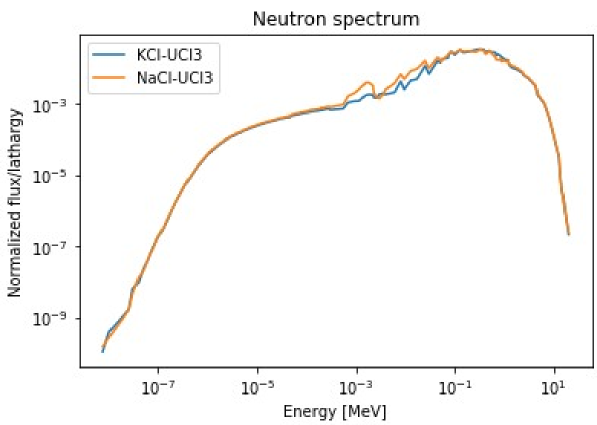

Figure 6. Salt-dependent neutron spectrum

Table 2. Comparison results of the two fuel salts

Fuel salt	Melting point	U-235 enrichment for criticality	Conversion Ratio
46KCl-54UCl_3	831K (558°C)	14.1 w %	0.610
67NaCl-33UCl_3	793K (520°C)	15.7 w %	0.575

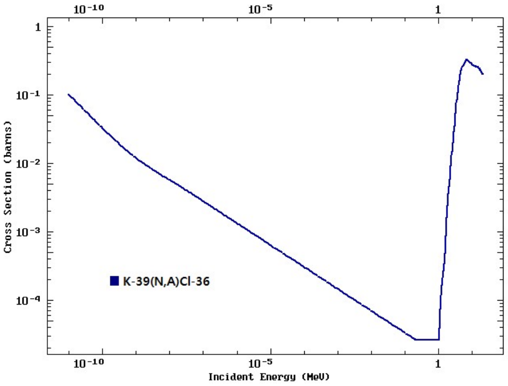

Figure 7. Cross section of K-39(n,alpha)Cl-36

The exploitation of KCl-UCl_3 insinuates the possibility of Cl-36 production, which stems from the n, alpha reaction of K-39. It is speculated that such an effect will be inconsequential due to negligibly small n, alpha cross section of K-39, which is shown in Fig. 7. Comprehensively, the higher solubility regarding UCl_3 for the KCl-UCl_3 system results in a lower enrichment of U-235 and higher conversion ratio. As a result, the KCl-UCl_3 system was recognized to be a more suitable fuel salt for the Molten Chloride Salt Fast Reactor.

2.4 Cl-37 enrichment

Figure 8 shows the capture cross section of Cl-35 and Cl-37. Note that Cl-35 has a larger capture cross section, and produces Cl-36 through n, gamma reaction. Hence, a concentration of Cl-37 directly enhances the neutron economy. Table 3 enumerates the variation in the Cl-37 concentration and its associated K_{eff} values. The concentration of 99 atomic percent was considered to be sufficient enough and employed throughout the study.

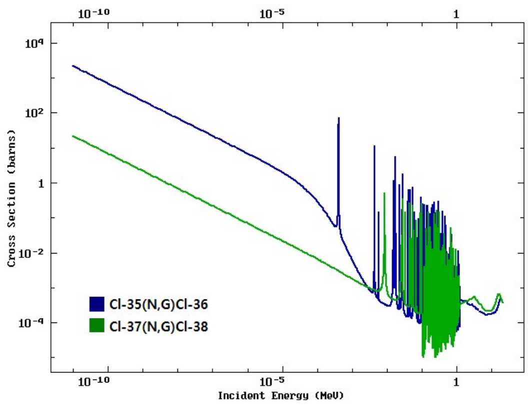

Figure 8. Capture cross section of Cl

Table 3. Impact of Cl-37 enrichment on the K_{eff} value

Cl-37 enrichment	K_{eff}
90%	0.99247 ± 0.00031
95%	0.99776 ± 0.00031
99% [Reference]	1.00203 ± 0.00033
99.9%	1.00229 ± 0.00031

3. Reactor properties

3.1 Reactivity control drum

Figure 9 shows the x-y plane of drum-type reactivity control devices, where total of 20 reactivity control drums are located in the stainless-steel reflector region. The net reactivity worth of the devices is about 3,500pcm as illustrated in Table 4.

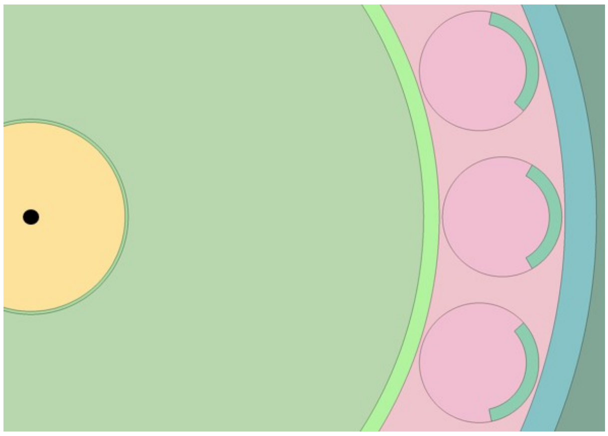

Figure 9. Configuration of the drum-type reactivity control device (X-Y plane)

Table 4. Impact of reactivity control drum

Status	K_{eff}
Drum out(Maximum reactivity)	1.00203 ± 0.00033
Drum in(Minimum reactivity)	0.96675 ± 0.00033

3.2 Burn up

To analyze the characteristics of the reactor, a burn up calculation was performed for 21 years with a prescribed reactor power of 400MWth.

Table 5 summarizes the excess reactivity of the core along with the increase of the burn up. Initial excess reactivity of 3,500pcm allows the operation for more than 18 years, and it shows a clear accumulation of Pu-239 with the increase in the burn up. It is worthwhile to mention that increase in the Pu fraction is beneficial since it lowers the melting temperature of the salt, which is shown in Fig. 3.

Table 6 enumerates the variation in the conversion ratio of the core with respect to the increase of the burn up. Note that due to the high eta value (η) of Pu, the increase in Pu has the effect of increasing the conversion ratio.

Table 5. Excess reactivity and accumulation of Pu-239

Years	Burn up (MWd/kgU)	K_{eff}	Excess reactivity	Pu-239 [ton]
0	0.00	1.03614 ± 0.00032	3,488	0.000
1	2.40	1.03454 ± 0.00031	3,339	0.089
3	7.19	1.03082 ± 0.00031	2,990	0.264
6	14.39	1.02601 ± 0.00032	2,535	0.519
9	21.58	1.02052 ± 0.00033	2,011	0.763
12	28.77	1.01551 ± 0.00034	1,528	0.997
15	35.95	1.00892 ± 0.00032	884	1.221
18	43.14	1.00432 ± 0.00033	430	1.434
21	50.32	0.99834 ± 0.00033	-166	1.637

Table 6. Conversion ratio

Years	Burn up (MWd/kgU)	CONVERSION RATIO
0	0.00	0.561 ± 0.00068
1	2.40	0.564 ± 0.00064
3	7.19	0.571 ± 0.00064
6	14.39	0.582 ± 0.00066
9	21.58	0.592 ± 0.00065
12	28.77	0.603 ± 0.00065
15	35.95	0.614 ± 0.00065
18	43.14	0.624 ± 0.00063
21	50.32	0.635 ± 0.00064

3.3 Power distribution

Figures 4 and 5 show radial and axial power distribution of active core. They show similar shape of the Bessel and cosine function, respectively. 97.77% of power were produced in the active core region.

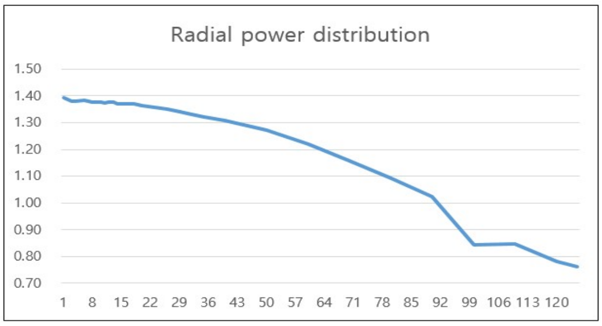

Figure 10. Radial power distribution

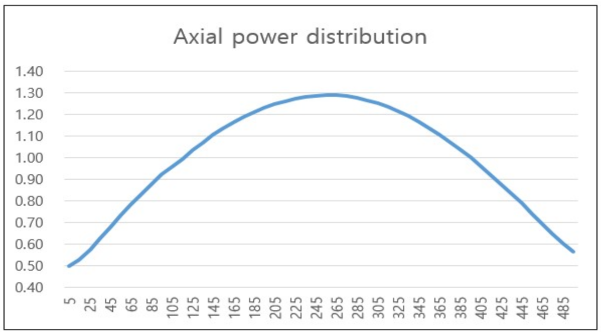

Figure 11. Axial power distribution

4. Conclusions

In order to overcome drawbacks of thermal neutron MSR, fast neutron MSRs are attracting attention. One of the potential nuclear fuel salts for the molten salt fast reactor, chloride based KCl-UCl_3 salts and NaCl-UCl_3 were studied. The NaCl-UCl_3 system has an advantage of lower melting point than the KCl-UCl_3 system. However, the KCl-UCl_3 system has higher solubility of UCl_3 than the NaCl-UCl_3 system at the eutectic temperature. Due to the high solubility of UCl_3 in the KCl-UCl_3 system, initial criticality can be met with a clearly lower U-235 concentration compared to the NaCl-UCl_3 system. A lower U-235 concentration of the KCl-UCl_3 system has higher conversion ratio. As a result, the KCl-UCl_3 system was determined to be a more suitable fuel salt for the Molten Chloride Salt Fast Reactor.

ACKNOWLEDGEMENTS

This work was supported by the National Research Foundation of Korea (NRF) Grant funded by the Korean Government (MSIP) (NRF-2016R1A5A1013919)

REFERENCES

[1] https://www.gen-4.org/

[2] L. Mathieu, D. Heuer, E. Merle-Lucotte et al., “Possible Configurations for the Thorium Molten Salt Reactor and Advantages of the Fast Non-Moderated Version”, Nucl. Sc. and Eng., 161, 78-89 (2009).

[3] S. GHOSH et al., “Experimental Investigations and Thermodynamic Modelling of KCl–LiCl–UCl3 System,” Calphad, 45, 11 (2014); https://doi.org/10.1016/j.calphad.2013.11.001.

[4] O. Benesˇ, R.J.M. Konings, "Thermodynamic evaluation of the NaCl–MgCl2–UCl3–PuCl3 system", Journal of Nuclear Materials 375 (2008) 202–208

[5] https://www-nds.iaea.org/exfor/endf.htm

[6] J. Leppanen, et al. "The Serpent Monte Carlo code: Status, development and applications in 2013." Ann. Nucl. Energy, 82 (2015) 142-150(https://montecarlo.vtt.fi/)